Electronic structure of a metal-semiconductor interface*

Steven G. Louie† and Marvin L. Cohen
Department of Physics, University of California, and Inorganic Materials Research Division, Lawrence Berkeley Laboratory, Berkeley, California 94720
(Received 25 August 1975)

The electronic structure of a jellium-Si interface is calculated using a jellium density corresponding to Al and self-consistent Si pseudopotentials. Local densities of states and charge densities are used to study states near the interface. At the Si surface, a high density of extra states is found in the energy range of the Si fundamental gap. These states are bulklike in jellium and decay into Si with a high concentration of charge in the dangling-bond free-surface-like Si state. Truly localized interface states are also found but at lower energies. The calculated barrier height is in excellent agreement with recent experimental results.

I. INTRODUCTION

In this paper we present self-consistent pseudopotential calculations on the electronic structure of a metal-semiconductor interface. The calculations model an Al-Si interface with a jellium potential representing the aluminum-ion potential in contact with the Si (111) surface. This model describes an ideal interface; i.e., there is no oxide layer between the two materials. A local density of states (LDOS) which displays the density of states as a function of distance away from the interface has been calculated for this Al-Si junction. Various states which exist near the interface are identified and discussed in terms of the LDOS and their charge densities. Our calculated interface barrier height is found to be in excellent agreement with recent experimental results.[1] To our knowledge, this is the first realistic self-consistent calculation for a metal-semiconductor interface.

Metal-semiconductor interfaces are of great importance because of their rectifying properties, which are crucial to the operation of many electronic devices. Many experimental efforts have been devoted to the study of their properties. With the advent of recent ultrahigh-vacuum techniques, ideal interfaces can now be fabricated and studied systematically,[1-5] and the detailed electronic structure at the interface can be probed using modern photoemission techniques.[3-5] On the theoretical side, metal-semiconductor interfaces have been the subject of much discussion and speculation.[6-15] Many models have been proposed to explain the interface properties. However, regrettably, past theoretical investigations into their electronic structure have been mostly qualitative or semiquantitative. A clear picture of the electronic structure at a metal-semiconductor interface has yet to emerge.

Experimentally, the electrical barrier height ϕ_B (Schottky barrier) at a metal-semiconductor interface can be accurately determined using many different methods (I-V, C-V, photoelectric, etc.). To avoid confusion over n- and p-type semiconductors, we measure here the barrier height from the Fermi level E_F to the semiconductor conduction band. For covalent semiconductors such as Si and Ge, the barrier height is found to be virtually independent of the metal contact and of the doping in the semiconductor.[1,15,16] Bardeen[6] attributed this behavior of the barrier height to a high density of surface states in the semiconductor band gap; i.e., the filling or emptying of these surface states pins the Fermi level to a nearly constant value. Heine,[7] on the other hand, pointed out that semiconductor surface states cannot exist in the semiconductor gap if this energy range is inside the metallic band. He suggested that the pinning of the Fermi level is due to states of a different type in the semiconductor gap. These states are composed of the states from the tails of the metallic wave functions decaying into the semiconductor side.

Theories[8,10-12] which do not explicitly involve extra states in the semiconductor gap have also been proposed to explain the barrier-height behavior. Inkson,[8,10] using a model-dielectric-function formulation, proposed that the pinning of the Fermi level is due to the narrowing of the semiconductor gap at the interface. According to Inkson, the screening of the valence and conduction bands of the semiconductor is different near the interface. This causes the valence band to bend up and the conduction band to bend down and eventually the bands merge together at the interface for a covalent semiconductor. In addition, Phillips[11,12] claimed that polarizability effects play the dominant role at the metal-semiconductor interface. He suggested that it is the elementary excitations[11] and chemical bonding[12] at the interface which determine the behavior of the Schottky barrier.

The purpose of the present work is to study the electronic structure of a metal-semiconductor interface in detail using the Al-Si junction as a pro-

totype and to gain some insights into the nature of metal-semiconductor Schottky barriers. The model and methods of calculation presented here can be applied to general metal-semiconductor contacts. The main features of this calculation which are absent in previous work are as follows: (i) A realistic interface is constructed through a jellium-semiconductor model and (ii) the calculation is self-consistent. It is noted that, as in all previously existing self-consistent surface calculations, self-consistency in the present context means self-consistency in the electronic responses to a given structural model.

The remainder of the paper is organized as follows: In Sec. II the model for the interface and the steps in the self-consistent calculations are discussed in detail. In Sec. III the results for the electronic structure of the Al-Si interface are presented. And in the final section, IV, some discussion and conclusions are presented.

II. CALCULATIONS

Our model for an ideal metal-semiconductor interface consists of jellium in contact with a semiconductor described in the pseudopotential formalism. Present experimental and theoretical methods do not allow a detailed determination of the geometry at the metal-semiconductor interface; however, we believe that the important properties of the interface are dominated by the properties of the free electrons residing next to the semiconductor surface. The present model is expected to contain all of the essential features of a metal-semiconductor interface.

The method we have employed to calculate the electronic structure of the Al-Si interface is similar to the method which we have used previously in surface and molecular calculations.[17–20] The main difficulties in calculating the electronic structure of solid interfaces are the following:

(i) Periodicity along the direction perpendicular to the interface is absent. Therefore the established methods for bulk calculations which depend on the periodicity of crystalline solids cannot be used.

(ii) Self-consistency is essential in obtaining realistic solutions. It is necessary to allow the electrons to react to the boundary conditions imposed by the interface and the resulting readjustment and screening is a fundamental part of the problem.

The essence of our method is to retain (artificial) periodicity perpendicular to the interface and thus allow the use of well-established tools in pseudopotential crystal calculations to calculate the interface electronic structure. In addition, the method goes beyond the usual pseudopotential approach through the requirement of self-consistency. This method has been successfully applied to surfaces[18–20] (both for metal and semiconductor surfaces) and molecular[17] calculations.

For the present calculation, we consider a unit cell consisting of a slab of Si with the (111) surfaces exposed to a jellium of Al density on both sides. This cell is then repeated and the electronic structure of the system is calculated self-consistently. The basic idea consists of considering periodic interfaces which are separated by large distances, and then obtaining the essential features of a single interface by calculating the electronic structure of this periodic system. The unit cell used consists of 12 layers of Si plus an equivalent distance of jellium. It is spanned in two dimensions by the shortest lattice vectors parallel to the Si (111) surface, i.e., hexagonal lattice vectors with length 7.26 a.u., and by a long c axis of length $c = 71.1$ a.u. The volume of the cell is equal to 3241 a.u.^{3}

With the above geometry, the jellium edge is one-half of a Si-Si bond length away from the atoms of the Si (111) surface. This is a physically reasonable choice since the length of an Al-Si bond is approximately the same as a Si-Si bond. To simulate noninteracting interfaces, the Si and the Al slab sizes have to be chosen such that (a) the bulk properties of the materials are adequately reproduced and (b) the surfaces from opposite sides of the same slab do not interact appreciably. Calculations on the Si (111) surface[18,19] and various test calculations on jellium slabs of Al density showed that the assumed slab thickness which is equivalent to 12 layers of Si satisfies the above requirements well.

The electronic structure of this "periodic" system can now be determined in a self-consistent manner using pseudopotentials. The steps leading to a self-consistent solution are shown in Fig. 1. We expand the electron wave functions in plane waves with reciprocal-lattice vectors $\vec{G}$:

$$\psi_{n\vec{k}}(\vec{r}) = \sum_{\vec{G}} a^n_{\vec{k}}(\vec{G})\, e^{i(\vec{k}+\vec{G})\cdot\vec{r}} . \qquad (1)$$

This leads to a matrix eigenvalue equation of the usual kind,

$$\sum_{\vec{G}'} (H_{\vec{G},\vec{G}'} - E\delta_{\vec{G},\vec{G}'})\, a_{\vec{k}}(\vec{G}') = 0 , \qquad (2)$$

which is solved by standard methods.[21] Here, the Hamiltonian matrix elements are of the form

$$H_{\vec{G},\vec{G}'} = (\hbar^2/2m)|\vec{k}+\vec{G}|^2 \delta_{\vec{G},\vec{G}'} + V_{ps}(\vec{G},\vec{G}') , \qquad (3)$$

where $V_{ps}(\vec{G},\vec{G}')$ are the pseudopotential matrix elements. In general the pseudopotentials are nonlocal and energy dependent.[21] However, for bulk Si and Si surfaces, local pseudopotentials are known to yield satisfactory results. Therefore

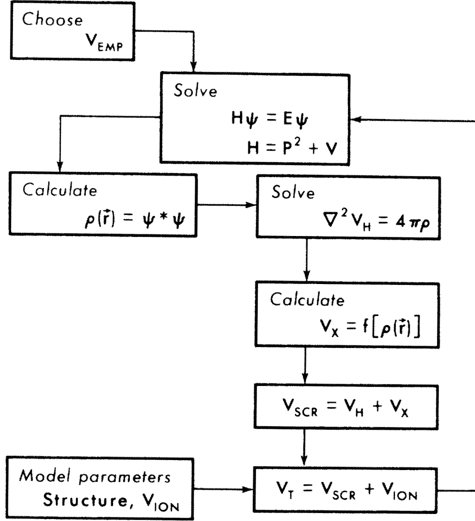

FIG. 1. Self-consistent loop in calculating the electronic structure of a metal-semiconductor interface.

local pseudopotentials will be used throughout for the present calculation.

The self-consistent cycle is initiated by the following potential:

$$V_{\text{start}}(\vec{G}) = S(\vec{G}) V^{\text{Si}}_{\text{emp}}(|\vec{G}|) + V^{\text{Al}}_{\text{start}}(\vec{G}) . \tag{4}$$

The first term is the starting potential for the Si slab and the second term is the starting potential for the Al slab. The Si structure factor

$$S(\vec{G}) = \frac{1}{M} \sum_{\tau_i}^{M} e^{-i\vec{G}\cdot\vec{\tau}_i} \tag{5}$$

describes the positions of the Si atoms in the unit cell. $V^{\text{Si}}_{\text{emp}}(|\vec{G}|)$ are Si atomic pseudopotential form factors derived from empirical bulk calculations.[22] Since empirical form factors are only known for discrete $\vec{G}$ vectors and the $\vec{G}$ vectors are different for different crystal structures, a continuous extrapolation is performed to obtain the form factors corresponding to the new $\vec{G}$ vectors in the interface problem. We fitted a curve of the form

$$V(q) = \frac{a_1(q^2 - a_2)}{e^{a_3(q^2 - a_4)} + 1} \tag{6}$$

to the three form factors for bulk Si, $V(111) = -0.2241$ Ry, $V(200) = 0.0551$ Ry, $V(311) = 0.0724$ Ry, and renormalized it for the different unit-cell volume. The four parameters a_i in Eq. (6) are given in Table I. The potential is normalized to an atomic volume of 270 a.u.[3] and the units are in Ry if q is entered in a.u.

A starting potential for the Al slab is less obvious. We assumed that in zeroth order, the Al electronic charge is uniform and confined completely inside the Al slab. Then the Hartree part of the electron screening will cancel the positive jellium background and the starting potential for the Al slab can be taken to contain only an exchange term

$$V^{\text{Al}}_{\text{start}}(\vec{G}) = -\alpha(3/2\pi)(3\pi^2)^{1/3} e^2 \rho^{1/3}_{\text{jel}}(\vec{G}) , \tag{7}$$

where $\alpha = 0.79$ and $\rho^{1/3}_{\text{jel}}(\vec{G})$ are the Fourier components of the jellium density to the one-third power. Here we have replaced the nonlocal Hartree-Fock exchange potential $V_x(r, r')$ by the statistical exchange model of Slater.[23] The choice of $\alpha = 0.79$ will be discussed later. In principle, for a self-consistent calculation, the starting potentials should be unimportant. However, in practice, a good starting potential reduces the number of iterations needed enormously.

From Eq. (2) we obtain the band structure $E_n(\vec{k})$ and the pseudo-wave-functions $\psi_{n\vec{k}}(\vec{r})$. To perform the next step in the self-consistent loop, the total valence charge density

$$\rho(\vec{r}) = 2 \sum_n \sum_{\vec{k}} \psi^*_{n\vec{k}}(\vec{r}) \psi_{n\vec{k}}(\vec{r}), \quad E_n(\vec{k}) \le E_F \tag{8}$$

has to be accurately determined. This requires good convergence in the electron wave functions and a precise location of the Fermi level. To assure good convergence, the electronic wave functions were expanded in a basis set consisting of approximately 270 plane waves. This expansion corresponds to a kinetic-energy cutoff[21] $E_1 = |\vec{G}_{\max}|^2 \approx 2.7$ Ry. In addition, another 300 plane waves were included via Löwdin's perturbation scheme.[21] The total valence charge density was evaluated at 21 $\vec{k}$ points in the irreducible part ($\frac{1}{12}$) of the *two*-dimensional hexagonal Brillouin zone, with the Fermi level determined by demanding charge neutrality in the unit cell. That is, the Fermi level is determined by filling the eigenlevels in the Brillouin zone until the number of occupied levels corresponds to the number of electrons in the unit cell required by charge neutrality.

We note that, for our "periodic" system, we should in principle evaluate the total charge over the whole three-dimensional Brillouin zone. However, for a large elongated cell, as in the present case, the energies and wave functions are quite independent of the component of the $\vec{k}$ vectors along the c direction. As we shall see later, the final

TABLE I. Parameters entering Eqs. (6) and (16) to define the empirical and ionic Si pseudopotentials.

	$V^{\text{Si}}_{\text{emp}}$	$V^{\text{Si}}_{\text{ion}}$
a_1	0.17459	−0.57315
a_2	2.22144	0.79065
a_3	0.86334	−0.35201
a_4	1.53457	−0.01807

charge density away from the interface is in accord with the bulk calculations, thus indicating that our sampling in $\vec{k}$ space is sufficiently fine and the wave functions are converged.

Once the valence charge density $\rho(\vec{r})$ is known in terms of its Fourier components $\rho(\vec{G})$, the Hartree-Fock-type screening potentials V_H and V_x can be evaluated easily. V_H, the so-called Hartree screening potential, is the repulsive Coulomb potential seen by an electron and is generated by all the valence electrons. It is related to the valence charge density by Poisson's equation

$$\nabla^2 V_H(\vec{r}) = -4\pi e^2 \rho(\vec{r}) \tag{9}$$

and can be written as a Fourier series

$$V_H(\vec{r}) = \sum_{\vec{G}} V_H(\vec{G})\, e^{i\vec{G}\cdot\vec{r}} , \tag{10}$$

with

$$V_H(\vec{G}) = 4\pi e^2 \rho(\vec{G})/|\vec{G}|^2 . \tag{11}$$

Physically, over-all charge neutrality in the solid requires that $V_H(\vec{G}=0) = -V_{\text{ion}}(\vec{G}=0)$, where V_{ion} is the ionic potential generated by the positive Si^{+4} ion cores and by the positive jellium slab. Therefore, for the present calculations, we can arbitrarily set $V_H(\vec{G}=0) = V_{\text{ion}}(\vec{G}=0) = 0$. Numerically, however, the divergent character of $V_H(\vec{G})$ and $V_{\text{ion}}(\vec{G})$ for small $\vec{G}$ values causes some problems with the stability of the self-consistency process. This is discussed in detail in Ref. 19. The Hartree-Fock exchange potential was approximated using the Slater exchange model, as we did for the Al starting potential. In $\vec{G}$ space, the exchange potential then has the form

$$V_x(\vec{G}) = -\alpha(3/2\pi)(3\pi^2)^{1/3} e^2 \rho^{1/3}(\vec{G}) , \tag{12}$$

where $\alpha = 0.79$ and $\rho^{1/3}(\vec{G})$ are Fourier components of $\rho^{1/3}(\vec{r})$. The justification for the present value for α is that this choice of α will bring Slater's exchange in an approximate agreement with Wigner's[24] interpolation formula at the average valence charge density of Al and Si. Thus, from the total charge density, the electronic screening potential

$$V_{\text{SCR}}(\vec{r}) = \sum_{\vec{G}} [V_H(\vec{G}) + V_x(\vec{G})]\, e^{i\vec{G}\cdot\vec{r}} \tag{13}$$

is obtained at each iteration in the self-consistent loop.

After the screening potential is determined, the self-consistent process is continued by adding V_{SCR} to an ionic potential V_{ion} to form a potential for the next iteration. The ionic potential consists of two terms,

$$V_{\text{ion}}(\vec{G}) = S(\vec{G})\, V^{\text{Si}}_{\text{ion}}(\vec{G}) + V^{\text{Al}}_{\text{ion}}(\vec{G}) , \tag{14}$$

where the first term is generated by the Si^{+4} ionic cores and the second term is generated by the Al slab. $S(\vec{G})$ is the Si structure factor as defined in Eq. (5).

First let us discuss $V^{\text{Al}}_{\text{ion}}$. This is just the Coulombic potential generated by repeated slabs of uniform positive charge. For an origin at the center of a metallic slab, $V^{\text{Al}}_{\text{ion}}$ has the form

$$V^{\text{Al}}_{\text{ion}}(\vec{G}) = \frac{-8\pi e^2 n_+ \sin G_z a/2}{C G_z^3}\, \delta_{G_x 0}\, \delta_{G_y 0} , \tag{15}$$

where a is the width of the jellium slab, C is the length of the unit cell along the direction (z) perpendicular to the interface, and n_+ is the positive background density.

For the Si-ion core potential, we have used an atomic model potential which was fitted to atomic term values by Abarenkov and Heine.[25] The repulsive cores of the ionic model potentials as given by Abarenkov and Heine are nonlocal (i.e., l dependent). For the present calculation, a local, "on the Fermi sphere" approximation[21] has been made and the Fourier transform of the resulting local potential was fitted to a four-parameter curve,

$$V^{\text{Si}}_{\text{ion}}(q) = (a_1/q^2)[\cos(a_2 q) + a_3]\, e^{a_4 q^4} . \tag{16}$$

The values of the a_i's are given in Table I. The normalization and the units for Eq. (16) are the same as those for Eq. (6). Using the parameters given in Table I, this ionic core potential has proven to yield excellent results in bulk and surface self-consistent calculations.[19]

With the above V_{ion}, the first two cycles of the self-consistent loop were performed using

$$V^{(1)}_{\text{IN}}(\vec{r}) = V_{\text{start}}(\vec{r}) ,$$
$$V^{(2)}_{\text{IN}}(\vec{r}) = V_{\text{ion}}(\vec{r}) + V^{(1)}_{\text{SCR}}(\vec{r}) . \tag{17}$$

However, owing to the divergent character of V_H and V_{ion} mentioned earlier, an input potential V_{IN} which deviates from the truly self-consistent potential will lead to an output potential which "overshoots" and is further away from the true potential. Therefore further iterations based on a straightforward extension of Eq. (17) would not yield a converging potential. This unstable behavior of the screening potential, especially for very small $\vec{G}$ vectors, is commonly found in surface calculations.[18–20,26,27] The procedure to deal with these instabilities is to compute adjusted input potentials $V^{(n)}_{\text{IN}}(\vec{G})$ for $n > 2$ from preceding input and output potentials. This can be done by obtaining the input potential of the nth iteration from a linear combination of input and output potentials of the $(n-1)$th iteration or from inspecting V_{OUT}-versus-V_{IN} graphs separately for each small $\vec{G}$. A detailed discussion of this problem and the procedures to overcome it are given in Ref. 19. The

criterion for self-consistency is now the stability of the adjusted input screening potential as compared to the output screening potential calculated from Eq. (13). In the present calculation, the final self-consistent potential is stable to within 0.01 Ry.

After self-consistency has been reached, the electronic structure of the interface can then be analyzed in terms of charge densities. For this purpose, charge densities have been calculated as a function of different energy intervals and different $\vec{k}$ points in the Brillouin zone. In addition, we performed a local density of states (LDOS) calculation for the Al-Si interface. This LDOS, which displays the density of states in real space, facilitates the identification and illustrates the characteristics of the various kinds of states at the interface. Analogous to the projected density of states in tight-binding calculations, the LDOS for a given region in real space is given by

$$N_i(E) = \sum_{\vec{k}_\parallel, n} \int_{\Omega_i} |\psi_{\vec{k}_\parallel, n}(\vec{r})|^2 \, d^3r \, \delta(E - E_n(\vec{k}_\parallel)) , \qquad (18)$$

where $\vec{k}_\parallel$ is the wave vector parallel to the interface, n is the band index, $\psi_{\vec{k}_\parallel, n}$ is the electronic wave function, and Ω_i is the volume of the chosen region. Physically $N_i(E)$ can be interpreted as the probability that an electron with energy E is found in the region i.

III. RESULTS

In this section our results for the Al-Si interface which have been briefly reported recently[28] are discussed. We find that four different types of states can exist near the Al-Si interface. Aside from the usual states which are bulklike in both materials, there are states with energy below the Al conduction band which are bulklike in the Si side but decay rapidly in the Al side. Also, in the two-dimensional Brillouin zone, we find extra "gap" states in the semiconductor energy gaps whenever the range of the gap is inside the metallic band. They are somewhat similar to the states suggested by Heine; i.e., they are bulklike in Al and decay rapidly in Si. However, at the Si surface, these gap states retain the characteristics of the "free-surface" Si *surface states* which existed in the absence of the metal. It is these states which pin the Fermi level and dominate the properties of the Al-Si junction. In addition, we find truly localized interface states which decay in both directions away from the interface. These appear in the Si energy gaps in the energy range below the Al conduction band.

First let us examine the total, self-consistent valence charge density. The total charge density is a good indicator of the quality of the present work. For the present calculations to adequately represent noninteracting interfaces, the charge densities away from the interface should resemble the bulk densities of the two materials. Figure 2 displays the total valence charge density in a (110) plane along with the function $\bar{\rho}_{\text{total}}(z)$, which is the total charge density averaged parallel to the interface with z being the direction perpendicular to the interface. For the purpose of discussing the charge densities and the local density of states, we have also divided the unit cell into 12 equal regions (slices) as shown partially in Fig. 2(b). The jellium edge is indicated by the double-dashed line. Only the charge within a few angstroms from the interface is significantly perturbed from the bulk values. The charge densities in regions I and II and regions V and VI are in accord with bulk densities.[22,29] The slight differences between the present Si charges away from the interface and those calculated in Refs. 22 and 29 are due to the difference in the cutoff energy E_1.

From Fig. 2(b) one sees the well-known Friedel oscillations in the Al charge density and there is a net transfer of charge from aluminum to silicon. On the Al side, regions I and II each contain 7.9% of the total charge in the unit cell, whereas region III contains only 7.6%. On the Si side, regions V and VI each contain 8.8% of the total charge but region IV contains 9.1%. Thus approximately 0.3% of the total charge in the unit cell has been transferred from region III to region IV. A dipole potential with an electric field pointing toward the Si side is hence set up at the interface. This is a consequence of equalizing the Fermi levels in the two materials. From Fig. 2(a), the Al charge appears to be spilling into the empty "channels" in the Si charge density and into the dangling-bond

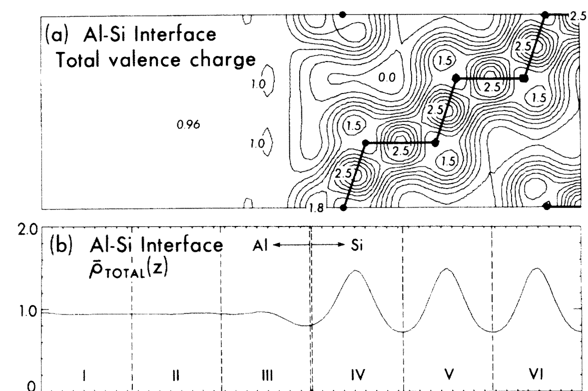

FIG. 2. (a) Total valence-charge-density contours in a (110) plane. The Si atoms are indicated by dots. (b) Total valence charge density averaged parallel to the interface and plotted along the direction perpendicular to the interface. The charge densities are normalized to 1 electron per unit cell.

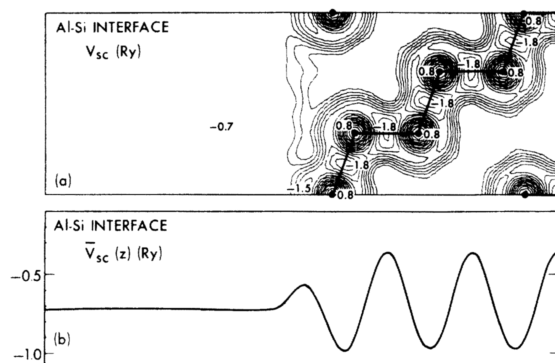

FIG. 3. (a) Contour plot of the final self-consistent potential V_{sc} in a (110) plane. (b) Final self-consistent potential averaged parallel to the interface and plotted along the direction perpendicular to the interface. The potential values are in rydbergs.

sites. The charge density at the dangling-bond sites in the present case is significantly higher than a sum of the jellium electron charge density and the Si charge density from the free-surface calculations. This indicates the formation of a metallic-covalent-like bond between Si and a jellium of Al density.

Figure 3 displays the self-consistent pseudopotential V_{sc} in a (110) plane along with $\bar{V}_{sc}(z)$, which is V_{sc} averaged parallel to the interface. The total charge density discussed earlier is the self-consistent response to this potential. The potential on the Al side is flat and does not show pronounced Friedel oscillations. Similar properties have been found in self-consistent calculations on the Al surface using the jellium model.[26] In the course of self-consistency, the Si potentials on the first two layers are made slightly deeper than the Si potentials further away from the interface. As expected, the perturbation to the Si potentials due to the presence of the metal appears to be much less than the perturbation due to the free surface.[19,30]

Now let us discuss the local density of states (LDOS) as defined in Eq. (18). We have calculated the LDOS for the six regions indicated in Fig. 2 by using 21 points in the irreducible part of the two-dimensional zone. The histograms of the LDOS for the six regions are shown in Fig. 4. To facilitate comparisons, the density of states of bulk Si from Ref. 22 is superimposed on the LDOS of regions IV–VI, and a free-electron density of states [i.e., $N(E)\sim E^{1/2}$] is superimposed on the LDOS of regions I–III. The Fermi level is indicated by the dashed line. Most of the interesting features appear in the LDOS of region IV. To investigate the energy positions of the extra states and their origins, we subtracted the LDOS of region VI from the LDOS of region IV to obtain a difference local density of states (DLDOS). The result is presented in Fig. 5. The positive portion of the histogram indicates an addition of states in that particular energy range in region IV and the negative portion of the histogram shows a depreciation of states.

The LDOS reveals much information about the electronic structure of the interface. From the position of the Fermi level and the position of the conduction-band edge of the semiconductor, one

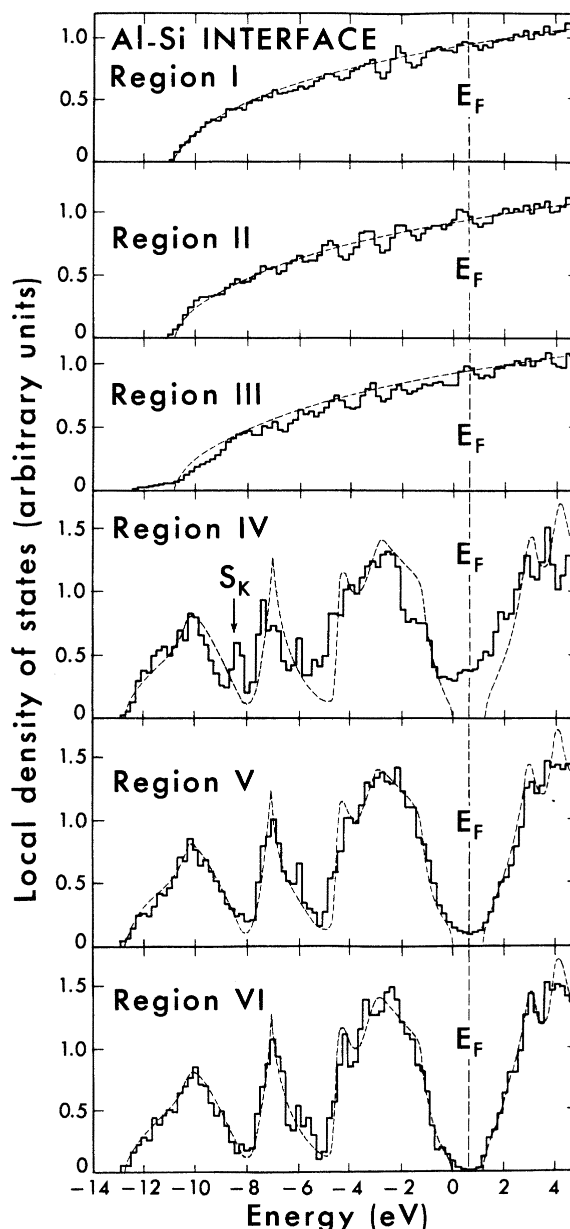

FIG. 4. Local density of states in arbitrary units as defined by Eq. (18). The regions are as shown in Fig. 2(b).

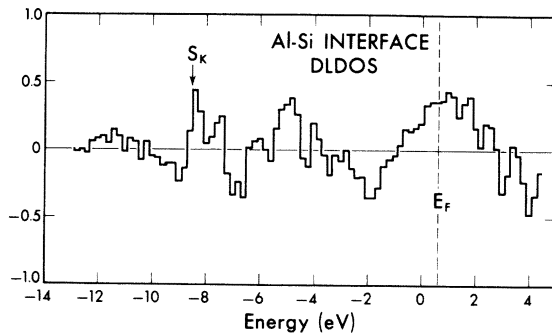

FIG. 5. Difference local density of states (DLDOS) obtained by subtracting the LDOS of region VI from that of region IV. The units are the same as in Fig. 4.

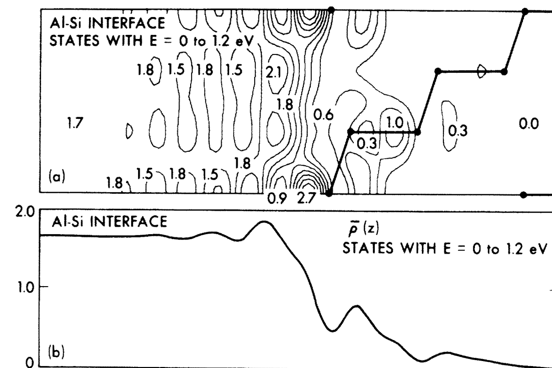

FIG. 7. (a) Charge-density contours for "gap" states with energy between 0 and 1.2 eV in the same plane and normalization as in Fig. 1(a). (b) Charge density in (a) averaged parallel to the interface and plotted along the direction perpendicular to the interface.

can calculate the barrier height at the interface. We obtained a barrier height of 0.6 ± 0.1 eV for the Al-Si interface, which is in excellent agreement with the recent experimental result[1] of 0.61 eV. There are other experimental values for the Al-Si barrier height, ranging from ~ 0.55 to ~ 0.70 eV. (See, for example, Ref. 15.) However, we believe that the value from Ref. 1 is the best for an ideal Al-Si interface because of the ultrahigh-vacuum conditions used in this particular experiment.

The various types of states which appear near the interface can be seen from the LDOS. States with energy below − 11.1 eV (i.e., below the onset of the Al conduction band) are bulklike in Si and do not penetrate into the bulk of Al. Of course there are states with higher energy which can behave similarly. For example, at the $\vec{k}$ point K, states with energy up to − 6.5 eV are below the Al conduction band. To illustrate this type of state, the charge density for all states with energy below − 11.5 eV is presented in Fig. 6. On the Si side, the charge-density contours strongly resemble the charge-density contours for the bottom band of bulk[22] Si whereas the charge on the Al side is completely zero.

From the LDOS of region IV (Fig. 4) or the DLDOS (Fig. 5), we see that the dips in the bulk Si density of states which are due to gaps in the Si band structure are being filled up by either interface states or "gap" states at the interface. The extra states centered at ~ − 8.2 eV are partially interface states and partially gap states, whereas the states centered at ~ − 5.0 eV and states in the optical gap are gap states.

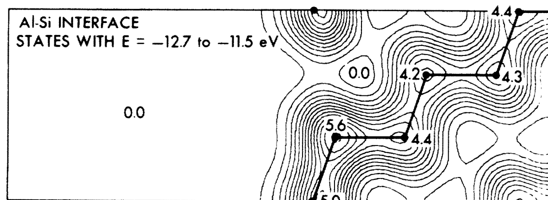

FIG. 6. Charge-density contours for states with energy below − 11.5 eV in the same plane and normalization as in Fig. 1(a).

The gap states in the optical gap are of particular importance because the density of these states sensitively influences the position of the Fermi level with respect to the semiconductor band edges. These states have a charge density which is metallic in the Al slab, becomes dangling-bond-like at the Si surface, and decays rapidly to zero in the Si slab. The charge density for these states in the thermal gap, i.e., states with energy between 0 and 1.2 eV, is plotted in Fig. 7 along with $\bar{\rho}(z)$, which is the same charge density averaged parallel to the interface. The dangling-bond surface states which exist at these energies for the free-surface case have been matched to the continuum of metallic states. Thus, as seen from Fig. 7(a), the charge is quite uniform in the Al slab but retains the dangling-bond character at the Si surface. We note that the charge density displayed in Fig. 7 is for all states with energy in the thermal gap. The decaying rates are different for states at different energies. The charge for states near midgap decays most rapidly into the Si side.

An examination of the LDOS of region IV from − 1.0 to 2.0 eV indicates that there is an apparent asymmetry in the distribution of extra states about the optical gap. A plausible physical explanation is the following: The states in the optical gap are derived from the valence band and the conduction band. Note the large depreciation of states near − 1.8 eV and near + 4.0 eV. (See Fig. 5.) Since

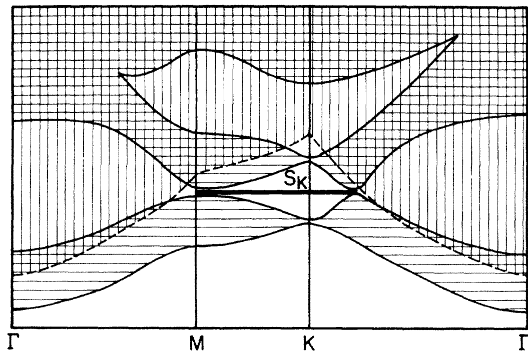

FIG. 8. Schematic diagram of the bottom two bands of the Si band structure (horizontally hatched) projected to the two-dimensional Brillouin zone. Superimposed on it is the projected Al conduction band (vertically hatched). S_K denotes the interface states discussed in the text.

these gap states are dangling-bond-like (i.e., p_z-like) in region IV and the top of the Si valence band is p-like, whereas the bottom of the conduction band is s-like, bulk states from the top of the valence band will be "robbed" to form the gap states while only states higher in the conduction band will be strongly affected by the formation of the gap states. Therefore the depreciation of bulk state densities will be larger at the top of the Si valence band than at the bottom of the conduction band. This results in the apparent asymmetry.

The interface states centered at -8.5 eV, labeled S_K in Fig. 4, appear near the point K in the two-dimensional hexagonal Brillouin zone. At first sight, localized states should not appear because there are aluminum states in this energy range. This appearance of interface states is a band-structure effect. Near the point K in $\vec{k}$ space, the Si two-dimensional band structure has a gap between -7.2 and -9.5 eV which is below the Al conduction band. In Fig. 8 we show a *schematic* diagram of the projected band structure of the bottom two bands of Si together with the projected band structure of Al. The Fermi levels of the two materials have been set equal. The lowest gap at K is the gap that we are discussing. Silicon surface states existing in this gap cannot be matched with any Al states because there are no Al states with the same energies and $\vec{k}$ vectors. A contour map of the charge density of the interface states at K at -8.5 eV is shown in Fig. 9. The charge density is s-like and highly localized on the outermost Si atoms. The charge is almost completely confined in region IV. Similar states with the same energy and character have been found in Si surface calculations. However the charge for states found in surface calculations is less localized.

IV. SUMMARY AND CONCLUSIONS

We have studied the electronic structure of a metal-semiconductor interface using an Al-Si system as a prototype. A jellium-semiconductor model has been constructed for the Al-Si interface. The electronic structure of the interface was then calculated using a method involving self-consistent pseudopotentials.[18] The model and methods of calculation used in the present paper have wider application than just the Al-Si system; these techniques can be extended straightforwardly to calculate the electronic structure of other metal-semiconductor interfaces.

Four different types of states are found to exist near the interface. The characteristics of these states have been analyzed in detail in terms of their charge densities. Our local-density-of-states results indicate a high density of "gap" states in the Si thermal gap near the Al-Si interface. This implies a pinning of the Fermi level by these gap states which is consistent with experimental results. It is important to note that, in the present calculation, we have used a statistical exchange model for the exchange potential. Hence both the valence bands and conduction bands see the same screening potential. Also, from examining the structure of the local density of states, there does not seem to be a merging of the valence band with the conduction band near the interface. Therefore, the pinning of the Fermi level can be explained without invoking Inkson's argument of merging of the bands due to the difference in the screening of the valence band and the conduction band at the interface. Furthermore, it is not very

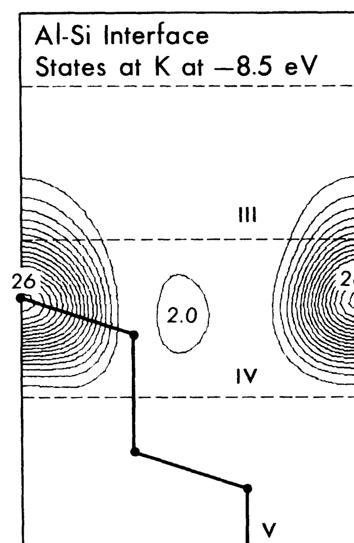

FIG. 9. Charge density contours for the interface states at K in the same plane and normalization as in Fig. 1(a).

meaningful to talk about a band picture as a function of distance away from the interface on such a microscopic scale.

The present calculation is for a high-density metal, Al, in contact with Si. For metals with a low density of s-p electrons, interface states can coexist with gap states in the energy range of the Si optical gap, such as in the -7.2- to -9.5-eV gap in the present calculation. Under such conditions, one expects that an even higher density of extra states will appear near midgap[18,19,30] and the Fermi level is again pinned in the thermal gap. This may be an explanation of why surface states continue to exist in the GaAs gap when an overlayer of[4,5] Cs or[3] Pd is placed on GaAs. Both Cs and Pd are metals of low s-p electron densities.

ACKNOWLEDGMENTS

The authors would like to thank Dr. F. Yndurain, Dr. M. Schlüter, and Dr. J. R. Chelikowsky for stimulating discussions. We would also like to thank Dr. Marc Brodsky for helpful conversations. Part of this work was done under the auspices of the U. S. Energy Research and Development Administration.

---

*Supported in part by the National Science Foundation under Grant No. DMR72-03206-A02.

†Supported by a National Science Foundation fellowship.

[1]A. Thanailakis, J. Phys. C 8, 655 (1975).

[2]A. Thanailakis, in Conference Series 22, *Metal-Semiconductor Contacts*, edited by M. Pepper (The Institute of Physics, London, 1974).

[3]J. L. Freeouf and D. E. Eastman, Phys. Rev. Lett. 34, 1624 (1975).

[4]W. E. Spicer, P. E. Gregory, P. W. Chye, I. A. Babalola, and T. Sukegawa, Appl. Phys. Lett. (to be published).

[5]P. E. Gregory and W. E. Spicer, Phys. Rev. B 12, 2370 (1975).

[6]J. Bardeen, Phys. Rev. 71, 717 (1947).

[7]V. Heine, Phys. Rev. 138, A1689 (1965).

[8]J. C. Inkson, J. Phys. C 5, 2599 (1972); 6, 1350 (1973).

[9]F. Yndurain, J. Phys. C 4, 2849 (1971).

[10]P. W. Anderson, in *Elementary Excitations in Solids, Molecules and Atoms, Part A*, edited by J. Devreese, A. Kunz, and T. Collins (Plenum, New York, 1974), p. 1.

[11]J. C. Phillips, Phys. Rev. B 1, 593 (1970).

[12]J. C. Phillips, J. Vac. Sci. Technol. 11, 947 (1974).

[13]A. J. Bennett and C. B. Duke, Phys. Rev. 160, 541 (1967); 162, 578 (1967).

[14]B. Pellegrini, Phys. Rev. B 7, 5299 (1973).

[15]S. M. Sze, *Physics of Semiconductor Devices* (Wiley, New York, 1969).

[16]S. Kurtin, T. C. McGill, and C. A. Mead, Phys. Rev. Lett. 22, 1433 (1969).

[17]M. L. Cohen, M. Schlüter, J. R. Chelikowsky, and S. G. Louie, Phys. Rev. B 12, 5575 (1975).

[18]M. Schlüter, J. R. Chelikowsky, S. G. Louie, and M. L. Cohen, Phys. Rev. Lett. 34, 1385 (1975).

[19]M. Schlüter, J. R. Chelikowsky, S. G. Louie, and M. L. Cohen, Phys. Rev. B 12, 4200 (1975).

[20]J. R. Chelikwosky, M. Schlüter, S. G. Louie, and M. L. Cohen, Solid State Commun. 17, 1103 (1975).

[21]M. L. Cohen and V. Heine, Solid State Phys. 24, 37 (1970).

[22]J. R. Chelikowsky and M. L. Cohen, Phys. Rev. B 10, 5095 (1974).

[23]J. C. Slater, Phys. Rev. 81, 385 (1951); W. Kohn and L. J. Sham, Phys. Rev. 140, A1133 (1965).

[24]E. P. Wigner, Phys. Rev. 46, 1002 (1934).

[25]I. V. Abarenkov and V. Heine, Philos. Mag. 12, 529 (1965).

[26]N. D. Lang and W. Kohn, Phys. Rev. B 1, 4555 (1970).

[27]G. P. Alldredge and L. Kleinman, Phys. Rev. B 10, 559 (1974).

[28]S. G. Louie and M. L. Cohen, Phys. Rev. Lett. 35, 866 (1975).

[29]J. P. Walter and M. L. Cohen, Phys. Rev. B 4, 1877 (1971).

[30]J. A. Appelbaum and D. R. Hamann, Phys. Rev. Lett. 32, 225 (1974).